Computational and Theoretical Chemistry 1040–1041 (2014) 35–44

Contents lists available at ScienceDirect

Computational and Theoretical Chemistry

journal homepage: www.elsevier.com/locate/comptc

A pair natural orbital based implementation of ADC(2)-x: Perspectives and challenges for response methods for singly and doubly excited states in large molecules

Benjamin Helmich, Christof Hättig *

Lehrstuhl für Theoretische Chemie, Ruhr-Universität Bochum, D-44780 Bochum, Germany

ARTICLE INFO

Article history:
Received 13 December 2013
Received in revised form 3 March 2014
Accepted 3 March 2014
Available online 12 March 2014

Keywords:
Pair natural orbitals
Excited states
ADC(2)-x
Coupled cluster
Double excitations

ABSTRACT

At the example of the extended algebraic-diagrammatic construction through second order, ADC(2)-x, we study the performance of a pair natural orbital (PNO) expansion for the description of partially or dominantly doubly excited states within a response theory framework. We find that with the presence of dominantly doubly excited states in the ADC(2)-x spectra the PNO truncation errors are between a factor of two and five larger than for strict second-order methods, where such excitations are only described in a zeroth-order approximation, but that otherwise the rate of convergence with the PNO selection threshold is similar.

Furthermore, we analyze the reason for the red shift of excitation energies in ADC(2)-x and trace it back to an unbalanced account of electron correlation effects in the ground and the excited state by the term added in the extended method to describe double excitations correct through first order. The balance can be restored by including the contributions from one additional commutator which accounts in lowest order for the coupling between double excitations in the ground and the excited state. A perturbative correction to ADC(2) which includes both correction terms for doubly excited configurations gives excitation energies close to results from CCSD with, however, much lower computational expenses.

The truncated pair natural orbital expansion for the ground and excited state doubles amplitudes opens a route to reduce the steep $\mathcal{O}(\mathcal{N}^6)$ cost-scaling of the extended ADC(2) and other higher-order response methods without significant degradation of their accuracy or a priori restriction of the double excitation manifold. Already our proof-of-principles implementation exhibits a cost-scaling between $\mathcal{O}(\mathcal{N}^3)$ and $\mathcal{O}(\mathcal{N}^4)$, which can be further reduced with a stringent use of integral screening and local density fitting to a quadratic cost-scaling.

© 2014 Elsevier B.V. All rights reserved.

1. Introduction

The advances made during the last two decades in response theory have promoted this approach from niche methods that were used only by a few specialized researchers to the most widely used tools used today for quantum chemical calculations of electronic spectra and structures and properties of excited states. The main trigger for these developments is that response theory allows to describe electronically excited states without requiring explicitly a multi-reference framework as long as the electronic ground state is suitable for a single-reference description. This opened a route to apply density functional theory (DFT) and efficient correlated single-reference wavefunction methods for the computation of excitation energies and spectra. Important for this progress have not only been the reduced computational costs which allowed applications on larger systems, but also the reduced complexity of the calculations, which permits to use these methods almost as black box, and of the implementations. The latter facilitated the development of a broad set of functionalities as e.g. analytic derivatives [1–6], cross sections for two-photon and other nonlinear spectroscopies [7–12], or non-adiabatic coupling constants [13–15].

At the DFT level modern response theory can nowadays be applied to systems with several hundreds of atoms. But also second-order correlated wavefunction methods as e.g. configuration interaction singles (CIS) with a perturbative doubles correction [16], CIS(D), the algebraic-diagrammatic construction through second order [17] (ADC(2)), and the approximate coupled cluster singles and doubles model [18] CC2 can be applied to systems with hundred and more atoms with modern integral- and

* Corresponding author.
E-mail addresses: benjamin.helmich@rub.de (B. Helmich), christof.haettig@rub.de (C. Hättig).

http://dx.doi.org/10.1016/j.comptc.2014.03.004
2210-271X/© 2014 Elsevier B.V. All rights reserved.

amplitude-direct implementations [19–23] which make use of techniques like the resolution-of-the-identity or density-fitting approximation for two-electron integrals and local truncations of doubles amplitudes based on expansions in projected atomic orbitals or (generalized) pair natural orbitals.

A remaining obstacle of these response methods is that they either describe doubly excited states not at all so that they are completely missing in the spectrum, as e.g. in TDDFT and CIS(D), or only to zeroth order in the fluctuation potential as in CC2 and the related strict ADC(2) method, which is also denoted as ADC(2)-s, or CIS with quasi-degenerate second-order perturbation corrections [24], CIS(D_∞). The neglect or simplified treatment of double excitations leads also for excited states with only a partial double excitation character, as they are frequently met beyond the lowest HOMO–LUMO transitions, to undesirably large errors.

Higher-order response methods, which describe also doubly excited states correct through first or second order in the fluctuation potential as e.g. CCSD or CC3, are already for medium-sized molecules rather costly because of the steep scaling of their operation counts with the system size $\mathcal{N}$ as $\mathcal{O}(\mathcal{N}^6)$ and $\mathcal{O}(\mathcal{N}^7)$. Attempts to reduce the steep scaling for response methods beyond CC2, e.g. for CCSD, by combining them with a local truncation of the double excitation manifold based on a projected atomic orbital (PAO) based representation [25,26] have been discontinued. A hurdle for the development of local response methods for electronic excitations with a reduced cost-scaling is that these methods describe the physical electronic excitation process itself, which is often non-local, and correlation effects in the excited state by a single set of parameters. This is a qualitative difference between the response theory approach and state-specific methods like multi-reference configuration interaction or perturbation theory, which construct initially a first-order wavefunction for the excited state and then describe with a separate set of parameters the local dynamic correlation effects. In response theory methods the double excitation amplitudes have—because of the combined description of correlation and physical excitation—often large non-local contributions. For PAO based local correlation methods the decision of including or excluding orbitals in the expansion of the double excitation manifold for a given pair of occupied orbitals i, j is taken at the level of atomic subsets and the non-local contributions that describe the physical excitation process make it difficult to achieve then a competitive computational efficiency without compromising on the accuracy for excitation energies.

A new perspective on this issue came recently into reach with the revival of pair natural orbital (PNO) based local correlation methods [27–29]. They differ in two aspects from PAO based methods which are very important for the combination with response theory: First of all, the construction of the PNOs from an initial approximate first-order guess for the doubles amplitudes allows to adapt and tune the PNOs to the physical processes that have to be described and, secondly, the decision of including PNOs for the double excitation manifold of a pair i, j is done on the level of individual orbitals. This approach, which was originally only developed for ground-state correlation energies, has recently been generalized [22,23] for the description of single excitation dominated transitions within a response theory framework with the second-order wavefunction methods CIS(D), ADC(2), and CC2. With generalized state-specific PNOs the doubles amplitudes for the excited state are described as compactly as the ground state amplitudes. Already with a first proof-of-principles implementation we achieved a reduction of the cost-scaling with the system size $\mathcal{N}$ to a range that is intermediate between $\mathcal{O}(\mathcal{N}^3)$ and $\mathcal{O}(\mathcal{N}^4)$ with an early break even point of PNO-CC2 with the efficient RI-CC2 implementation.

The aim of the current work is to investigate the performance of truncated PNO expansions for the doubles amplitudes in response calculations with wavefunctions methods beyond CC2 and to analyze in particular the perspectives and challenges of this approach for excited states with a non-negligible or even predominant double excitation character. As guinea pig method for this investigation we have chosen the extended version of the algebraic-diagrammatic construction through second order ADC(2)-x. It was developed by Trofimov and Schirmer [30] as extension to ADC(2) which for excitation energies of doubly excited states is correct through first order in the fluctuation potential. ADC(2)-x was recently advocated by Starcke et al. [31] for the description of the low-lying doubly excited states in long polyene chains and by Knippenberg et al. [32] for polyacenes and their radical cations, which have also low-lying states with large doubly excited contributions.

In the following section we summarize the theory for ADC(2)-x in a pair natural orbital basis and the procedure for the construction and selection of the pair natural orbitals for excited states. The computational details for the validation of the computational performance of PNO-ADC(2)-x and its comparison to a canonical implementation and as well as for benchmark calculations with a standard test set for singlet excitations are specified in Section 3. The results of these calculations are presented and discussed in Sections 4 and 5. In Section 6 we analyze the origin of a large systematic red shift in the ADC(2)-x excitation energies and devise a perturbative doubles correction to ADC(2)-s which includes an additional coupling term for a more balanced account of correlation effects in the excited and the ground state. This perturbative doubles correction gives excitation energies close to the results from CCSD response theory, but has much lower computational costs. Finally, we conclude the article in Section 7 with a brief summary.

2. ADC(2)-x in a pair natural orbital basis

The ADC(2)-x excitation energies are obtained as eigenvalues of the secular matrix [30]:

$$\mathbf{M}^{\mathrm{ADC(2)-x}} = \begin{pmatrix} \widehat{S}_{\mu_1\nu_1}\langle\mu_1|[H+[H,T_2],\tau_{\nu_1}]|\mathrm{HF}\rangle & \langle\mu_1|[H,\tau_{\nu_2}]|\mathrm{HF}\rangle \\ \langle\mu_2|[H,\tau_{\nu_1}]|\mathrm{HF}\rangle & \langle\mu_2|[H,\tau_{\nu_2}]|\mathrm{HF}\rangle \end{pmatrix}, \tag{1}$$

where $\widehat{S}_{\mu\nu}$ is a symmetrization operator defined by $\widehat{S}_{\mu\nu}f_{\mu\nu} = \frac{1}{2}(f_{\mu\nu}+f^*_{\nu\mu})$ and T_2 are the first-order ground state doubles amplitudes. We assume an orthonormal operator and projection manifold for the single (μ_1) and double (μ_2) excitation spaces with $\langle\mu_i|\nu_j\rangle = \delta_{\mu_i,\nu_j}$ and $|\nu_j\rangle = \tau_{\nu_i}|\mathrm{HF}\rangle$ and $\langle\mu_i| = \langle\mathrm{HF}|\tau^\dagger_{\mu_i}$. The secular matrix $\mathbf{M}^{\mathrm{ADC(2)-x}}$ is then hermitian and, in contrast to the Jacobi matrix, which is used in coupled cluster response theory, its eigenvalues are guaranteed to be real. With real orbitals (which we assume in the following) the left and right eigenvectors are identical, otherwise they are the complex conjugate of each other.

For an iterative (“direct”) diagonalization without storage of the secular matrix we need to implement linear transformations of a trial vector $\mathbf{b}$ with $\mathbf{M}$. With the auxiliary operators $\hat{b}_i = \sum_{\mu_i} b_{\mu_i}\tau_{\mu_i}$, the result vector of such a transformation can be expressed as

$$\sigma_{\mu_1} = \langle\mu_1|[H,\hat{b}_1+\hat{b}_2]|\mathrm{HF}\rangle + \frac{1}{2}\langle\mathrm{HF}|\tau^\dagger_{\mu_1}[[H,T_2],\hat{b}_1] + \hat{b}^\dagger_1[[H,T_2],\tau_{\mu_1}]|\mathrm{HF}\rangle, \tag{2}$$

$$\sigma_{\mu_2} = \langle\mu_2|[H,\hat{b}_1+\hat{b}_2]|\mathrm{HF}\rangle. \tag{3}$$

In the pair natural orbital implementation T_2 is expanded in ground state PNOs and b_2 and σ_2 in a state-specific excited state PNO basis (vide infra) for the virtual space, while a localized molecular orbital (LMO) basis is used for the occupied space. In such a basis the

number of significant doubles amplitudes grows for the ground state (i.e. T_2) only linearly with the system size and for excited states (i.e. b_2 and σ_2) only linearly with the size of the chromophore(s) on which the excitation takes place, as demonstrated in our previous work [22].

To decrease the cost-scaling of the PNO construction, orbital specific virtual orbitals (OSVs) [33] were employed to build PNOs in a truncated virtual basis [23,34,35]. For the ground state, the coefficients $L_{b\tilde{c}_i}$ for the OSVs $\tilde{c}_i$ of an occupied LMO i are obtained from an eigenvalue decomposition of the pair contributions to the one-electron density matrix, from the diagonal pairs ii.

$$D^{ii}_{ab} = 4t^{ii}_{ac}\ t^{ii}_{bc} = L_{a\tilde{c}_i} n_{\tilde{c}_i} L_{b\tilde{c}_i}. \tag{4}$$

Here and in the following, we use the convention that $i, j, \ldots$refer to (active) occupied LMOs and $a, b, \ldots$to virtual canonical molecular orbitals. The densities are computed from approximate doubles amplitudes obtained as

$$t^{ii}_{ab} \approx \frac{K^{ii}_{ab}}{2\ F_{ii} - \varepsilon_a - \varepsilon_b}, \tag{5}$$

where K^{ii}_{ab} are electron repulsion integrals (ERIs), ε_a and ε_b canonical orbital energies, and F_{ii} diagonal Fock matrix elements. The four-index ERIs are calculated using the resolution-of-the-identity (RI) or density-fitting (DF) approximation with a Coulomb metric, [36,37]

$$K^{ii}_{ab} = \sum_Q B_{Q,ai} B_{Q,bi}, \tag{6}$$

$$B_{Q,ai} = \sum_P [\mathbf{V}^{-1/2}]_{QP} (P|ai), \tag{7}$$

where $(Q|ai)$ are three-index and $V_{PQ} = (P|Q)$ two-index electron repulsion integrals and P, Q auxiliary basis functions. For a given LMO i all those OSVs are discarded for which the occupation numbers $n_{\tilde{c}_i}$ are below a pre-defined threshold T_{OSV} (see Section 3 for details).

For excited states the approximate MP1 doubles amplitudes t^{ii}_{ab} in Eq. (4) are replaced by amplitudes [23]

$$b^{ii}_{ab} = \frac{K^{ii}_{ab} + \overline{B}_{Qai}\overline{B}_{Qbi}}{2\ F_{ii} + \omega - \varepsilon_a - \varepsilon_b}, \tag{8}$$

$$\overline{B}_{Q,ai} = \sum_{\mu\nu P} [\mathbf{V}^{-1/2}]_{QP} (P|\mu\nu) \left(\bar{\Lambda}^p_{\mu a} C_{\nu i} + C_{\mu a} \bar{\Lambda}^h_{\nu i} \right), \tag{9}$$

with the MO coefficients $C_{\alpha p}$ and the transformation matrices $\bar{\Lambda}^p_{\alpha a} = -C_{\alpha i}\ b_{ai}$ and $\bar{\Lambda}^h_{\alpha i} = C_{\alpha a}\ b_{ai}$. The parameter ω is a current approximation to the excitation energy.

Once the OSV coefficients $L_{a\tilde{a}_i}$ are available for all LMOs the three-index integrals are transformed into the OSV basis and further contracted to four-index ERIs in the direct OSV approximation [33] $K^{ij}_{\tilde{a}_i\tilde{b}_j}$ for the ground state and to

$$\overline{K}^{ij}_{\tilde{a}_i\tilde{b}_j} = \widehat{P}^{ij}_{\tilde{a}_i\tilde{b}_j}\ \overline{B}_{Q\tilde{a}_i i} B_{Q\tilde{b}_j j}, \tag{10}$$

for excited states with $\widehat{P}^{ij}_{ab} f^{ij}_{ab} = f^{ij}_{ab} + f^{ji}_{ba}$. With these two-electron integrals $K^{ij}_{\tilde{a}_i\tilde{b}_j}$ and $\overline{K}^{ij}_{\tilde{a}_i\tilde{b}_j}$ we estimate the second-order pair contribution to the correlation energy $e^{ij,(2)}$ and excited state doubles correction $\omega^{ij,(2)}_{es}$ by an approximation which is inspired by the scaled opposite spin methods [35,38,39]:

$$e^{ij,(2)} \approx \frac{c_{\mathrm{OS}}}{2} \sum_{\tilde{a}_i\tilde{b}_j} \frac{\left(K^{ij}_{\tilde{a}_i\tilde{b}_j}\right)^2}{F_{ii} - F_{\tilde{a}_i\tilde{a}_i} + F_{jj} - F_{\tilde{b}_j\tilde{b}_j}}, \tag{11}$$

$$\omega^{ij,(2)}_{es} \approx \frac{c_{\mathrm{OS}}}{4} \sum_{\tilde{a}_i\tilde{b}_j} \frac{\left(\overline{K}^{ij}_{\tilde{a}_i\tilde{b}_j}\right)^2}{F_{ii} - F_{\tilde{a}_i\tilde{a}_i} + F_{jj} - F_{\tilde{b}_j\tilde{b}_j} + \omega}. \tag{12}$$

As in SOS-ADC(2) and SOS-CC2 [40] we set the scaling factor to the standard value for SOS-MP2 [38] $c_{\mathrm{OS}} = 1.3$. The energy estimates in Eq. (11) and (12) are used to discard pairs with $e^{ij,(2)}$ or $\omega^{ij,(2)}_{es}$ that are smaller than a pair threshold T_{pair} (see Section 3 for details). Only for selected pairs with energy estimates above T_{pair} the OSV sets $\tilde{a}_i$ and $\tilde{b}_j$ are merged to an orthonormal and quasi-canonical pre-PNO basis $\tilde{a}_{ij}$, where $F_{\tilde{a}_{ij},\tilde{b}_{ij}} = \delta_{\tilde{a}_{ij},\tilde{b}_{ij}} \varepsilon_{\tilde{a}_{ij}}$ to simplify the computation of $t^{ij}_{\tilde{a}\tilde{b}}$ in Eq. (13) below. To obtain the final PNOs, we compute for each selected pair ij approximate double excitation amplitudes in the pre-PNO basis as

$$t^{ij}_{\tilde{a}\tilde{b}} = \frac{K^{ij}_{\tilde{a}\tilde{b}}}{F_{ii} + F_{jj} - \varepsilon_{\tilde{a}_{ij}} - \varepsilon_{\tilde{b}_{ij}}}, \tag{13}$$

and diagonalize the corresponding pair contribution to the correlated density:

$$D^{ij}_{\tilde{a}\tilde{b}} = 2\left(t^{ij}_{\tilde{a}\tilde{c}} t^{ij}_{\tilde{b}\tilde{c}} + t^{ij}_{\tilde{a}\tilde{c}} t^{ij}_{\tilde{b}\tilde{c}} \right) = d^{ij}_{\tilde{a}\tilde{c}} n^{ij}_{\tilde{c}} d^{ij}_{\tilde{b}\tilde{c}}. \tag{14}$$

Again, the eigenvectors $d^{ij}_{\tilde{a}\tilde{c}}$ with occupation numbers $n^{ij}_{\tilde{c}}$ below a selection threshold T_{PNO} are discarded. The remaining PNOs $\bar{a}_{ij}$ are then transformed into a quasi-canonical form with $F_{\bar{a}_{ij},\bar{b}_{ij}} = \delta_{\bar{a}_{ij},\bar{b}_{ij}} \varepsilon_{\bar{a}_{ij}}$ as described e.g. by Neese et al. [28].

For excited states the PNOs are generated in a similar way but with the approximate MP2 amplitudes $t^{ij}_{\tilde{a}\tilde{b}}$ in Eq. (14) replaced by approximated CIS(D)-like amplitudes in the pre-PNO basis:

$$b^{ij}_{\tilde{a}\tilde{b}} \approx \frac{\overline{K}^{ij}_{\tilde{a}\tilde{b}}}{\omega + F_{ii} + F_{jj} - \varepsilon_{\tilde{a}_{ij}} - \varepsilon_{\tilde{b}_{ij}}}. \tag{15}$$

The current approximation for single excitation amplitudes and the excitation energy ω enter in the ERIs $\overline{K}^{ij}_{\tilde{a}\tilde{b}}$ and the denominator of Eq. (15), respectively.

A special situation arises for charge-transfer (CT) excitations. For these states an important class of pairs has only very few PNOs with, however, large contributions to the excited state correlation energy $\omega^{(2)}_{es}$. This makes the PNO construction sensitive to the errors in the amplitudes which are caused by neglecting the off-diagonal elements of the Fock matrix in the LMO basis F_{ij} in Eq. (15) (cmp. Ref. [23]). These pairs are automatically recognized by a criterion described in Ref. 23 and the off-diagonal Fock matrix elements are included through a numerical Laplace transformation [41,42] of the denominator of Eq. (15), which can formally be written as

$$b^{ij}_{\tilde{a}\tilde{b}} \approx \widehat{P}^{ij}_{\tilde{a}\tilde{b}} \sum_{Qz} w_z \left(\sum_{i'a} B_{Qai'} X^z_{ii'} Y^z_{\tilde{a}a} \right) \left(\sum_{j'b} \overline{B}_{Qbj'} X^z_{jj'} Y^z_{\tilde{b}b} \right), \tag{16}$$

$$X^{(z)}_{ii'} = T_{ij}\ e^{-(\varepsilon_j + \frac{\omega}{4})\ t_z}\ T_{ij}, \tag{17}$$

$$Y^{(z)}_{\tilde{a}a} = d^{ij}_{\tilde{a}i} e^{(\varepsilon_a - \frac{\omega}{4}) t_z}, \tag{18}$$

where w_z and t_z are the Laplace weights and exponents, respectively, and T_{ij} the transformation matrix between LMOs and canonical occupied MOs. The numerical quadrature is performed every time excited state PNOs are constructed. The accuracy of the numerical quadrature is coupled to the threshold T_{PNO} (for further details we refer to Ref. 23). By performing a numerical Laplace transformation for selected pairs, a balanced accuracy with respect to PNO truncation is achieved for both local and CT excitations.

We note that the cost-scaling for building PNOs can be reduced by employing local subsets of the auxiliary basis functions. Further advances in the efficiency of the PNO construction involve either iterative diagonalization of the densities in Eq. (4) or the introduction of PAOs and truncated pair lists into the OSV and PNO construction, respectively [43,44].

In a previous work [23] we have reported the implementation of the linear transformations and the solution of the eigenvalue problem in a state-specific PNO basis for the CC2 model. As

described in Ref. 23, we obtained thereby also an implementation of the strict ADC(2)-s method by replacing the CC2 ground state amplitudes by the first-order amplitudes and $\langle HF|\tau^{\dagger}_{\mu_1}[[H,T_2],b_1]|HF\rangle$ by the symmetrized second term in Eq. (2) which required only minor modifications.

For the PNO implementation of the extended ADC(2)-x method, which is able to describe double excitations correct through first order in the fluctuation potential, we combined the PNO-ADC(2)-s code from Ref. 23 with routines developed originally to compute the MP2 residual $\langle\mu_2|[H-F,T_2]|HF\rangle$ for PNO-MP3(F12) [35]. To evaluate instead of the MP2 residual the contributions to the linear transformed trail vectors $\sigma_{\mu_2}=\langle\mu_2|[H-F,b_2]|HF\rangle$, that appear in ADC(2)-x in addition to the terms that are already present in ADC(2), we essentially had to replace T_2 and the ground state PNOs by the doubles parts of the trial vectors and the corresponding state-specific excited state PNOs, respectively. In the spin-orbital formulation the resulting expressions are:

$$\sigma^{ij}_{\bar{a}_{ij}\bar{b}_{ij}}=\hat{P}_{\bar{a}_{ij}\bar{b}_{ij}}\hat{P}_{ij}\sum_{k\bar{c}_{jk}}\left(K^{ik}_{\bar{a}_{ij}\bar{c}_{jk}}-J^{ik}_{\bar{a}_{ij}\bar{c}_{jk}}\right)b^{kj}_{\bar{c}_{kj}\bar{b}_{kj}}S^{kj,ij}_{\bar{b}_{kj}\bar{b}_{ij}}+\sum_{\bar{c}_{ij}>\bar{d}_{ij}}K^{\bar{c}_{ij}\bar{d}_{ij}}_{\bar{a}_{ij}\bar{b}_{ij}}b^{ij}_{\bar{c}_{ij}\bar{d}_{ij}}+\sum_{k>l}\sum_{\bar{a}_{kl}}S^{ij,kl}_{\bar{a}_{ij}\bar{a}_{kl}}\sum_{\bar{b}_{kl}}S^{ij,kl}_{\bar{b}_{ij}\bar{b}_{kl}}K^{ij}_{kl}b^{kl}_{\bar{a}_{kl}\bar{b}_{kl}}. \quad (19)$$

In the last equation $\bar{a}_{ij}$ denote excited state PNOs for a pair ij, $J^{ik}_{\bar{a}_{ij}\bar{c}_{jk}}$ are the Coulomb integrals $(ik|\bar{a}_{ij}\bar{c}_{jk})$, and $S^{ij,kl}_{\bar{a}_{ij}\bar{a}_{kl}}=\langle\bar{a}_{ij}|\bar{a}_{kl}\rangle$ are overlap integrals in the excited state PNO basis. Note that only pairs ij contribute to this expansion where both LMOs are located at or close to the chromophore(s) that contribute to the excitation and that the number of PNOs for a given pair becomes already for medium-sized molecules independent from system size and decreases with the distance between the centers of i and j. This leads for localized excitations in large molecular systems to a number of elements in $b^{ij}_{\bar{a}_{ij}\bar{b}_{ij}}$ and $\sigma^{ij}_{\bar{a}_{ij}\bar{b}_{ij}}$ which increases only sub-linearly with the system size. Consequently, also the operation count for the contractions in Eq. (19) will scale sub-linearly for such excitations. For excitations which are delocalized over the whole system the number of elements in the doubles part of the trial and result vectors grows linearly with the system size as shown in Ref. [22]. In our current proof-of-principles implementation we still accept a cubic cost-scaling [35] for the integrals in Eq. (19) and quartic scaling costs [23] for some contributions to σ_1.

3. Computational details

The PNO-ADC(2)-x method described in the previous section has been implemented in a development version of the TURBOMOLE program package [45]. As in our previous work [22,23], we used the same threshold T_{PNO} for the selection of ground and excited state PNOs. The pair selection threshold has for the calculations reported below been set conservatively to $T_{pair}=T_{\mathrm{PNO}}$ and the threshold for discarding OSVs to $T_{\mathrm{OSV}}=0.1T_{\mathrm{PNO}}$ as described in Ref. [23,35].

For the occupied orbital space we used Pipek-Mezey [46] localized molecular orbitals, which usually lead to the most compact PNO space for excited states [22]. CIS excitation energies and singles eigenvectors were used as initial guess for the excited state PNO construction. The CIS singles eigenvectors and corresponding CIS(D) doubles amplitudes were taken as start vectors for the Davidson procedure. Excited state PNOs were reconstructed with the current singles parts of the eigenvectors and the current excitation energies when $1-|\mathbf{E}^0\cdot\mathbf{E}|>\max\left(\beta\cdot\|\rho\|,\sqrt{T_{\mathrm{PNO}}}\right)$, where ρ is the current residual of the eigenvalue equation and $\mathbf{E}$ the current solution and $\mathbf{E}^0$ the initial guess for the eigenvector. We chose $\beta=10$ for the PNO-ADC(2)-x calculations to reduce to number of PNO re-constructions. They involve the re-computation of three-index and two-electron integrals in the new excited state PNO basis and are the most time-determining steps in the excitation energy computation.

Hartree–Fock calculations were carried out with the dscf program and canonical reference calculations with the methods ADC(2)-s, ADC(2)-x, CC2, and CCSD with the ricc2 program of the TURBOMOLE package [47]. For this purpose, the iterative ADC(2)-x and the perturbative ADC(2)-(x) and ADC(2)-(d) methods were implemented in the ricc2 module of a development version of the TURBOMOLE program package. For all excitation energies of states that are part of the benchmark set of the Thiel group [48,49], we employed the TZVP orbital basis set [50] and the corresponding optimized auxiliary basis set [51]. Excitation energies of polyenes were computed with the def2-TZVP basis set [51]. For all second row elements we froze the $1s^2$ core electrons.

For evaluating the additional errors introduced by the truncated PNO expansion in PNO-ADC(2)-x and the performance of the underlying ADC(2)-x method itself we used a large test set taken from the work of Schreiber et al. [48] which consists of 102 singlet excitations in 28 medium-sized organic molecules including conjugated hydrocarbons, aldehydes, amides, and a variety aromatic heterocycles. The structures of this benchmark set were taken from the Supplementary material of Ref. [48]. Tests for the computational performance of the PNO implementation were done on a series of conjugated polyenes. Their structures are specified in the Supplementary material of Ref. [22].

4. Performance of the PNO implementation of ADC(2)-x

An important question for the performance of PNO-based methods is the convergence of the results with the truncation threshold for the PNO expansion, T_{PNO}. For practical applications it should be chosen tight enough so that the PNO implementation has essentially the same accuracy (w.r.t. to the full configuration interaction limit) as conventional implementations. On the other hand, the computational savings that can be realized with a PNO-based implementation decrease soon with the tightness of T_{PNO}. Thus, one would like to avoid thresholds that are tighter than necessary.

We investigated the convergence of the PNO-ADC(2)-x results for vertical excitation energies for the test set developed by Schreiber et al. [48], which contains a large variety of different excitations in organic dyes including $\pi\pi^*$, $n\pi^*$, Rydberg, and mixed valence-Rydberg excitations. This test set also includes a number of transitions which are dominated by double excitations or are of mixed singly and doubly excited character. The results from this convergence study are compiled in Fig. 1, where we included for comparison the results for the PNO implementations of CIS(D) and CC2. (Results for ADC(2)-s are not shown because they are very similar to those for CC2.) The mean and maximum absolute errors in the excitation energies for PNO-ADC(2)-x are in the range of thresholds which is of interest for applications, $10^{-6}\geqslant T_{\mathrm{PNO}}\geqslant 10^{-9}$, between a factor of 2–5 larger than for the strict second-order methods. This increase of the PNO truncation error is surprisingly low considering that the generation of the PNOs and their iterative improvement only uses the single excitation part of the eigenvectors, which gives it only a limited flexibility to respond to large double excitation contributions in an excited state. In fact, we observe the largest truncation errors often not for those states with a large double excitation contribution but for single excitation dominated states which are energetically close to a double excitation in the same irreducible representation of the molecular point group.

An additional feature which contributes to the increased truncation errors for PNO-ADC(2)-x is that the fortunate cancellation of errors from the PNO truncation of the eigenvectors against those introduced by the PNO truncation of the ground state doubles

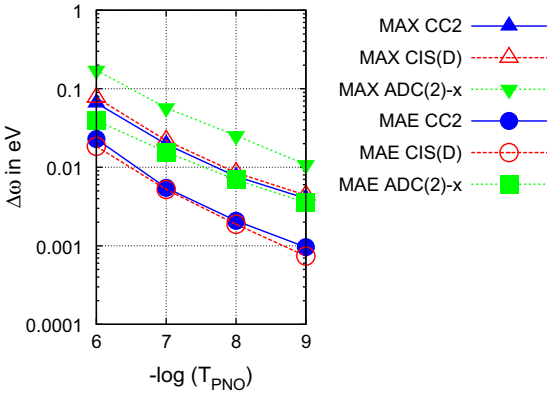


Fig. 1. Convergence of the truncation errors $\Delta\omega$ for PNO-CIS(D)/TZVP, PNO-CC2/TZVP, and PNO-ADC(2)-x/TZVP. For details of the test set see text. MAX is the maximum and MAE the mean absolute error.

amplitudes (cmp. discussion in Refs. [22,23]) happens for ADC(2)-x not to the same extent as for CIS(D), ADC(2), and CC2 because the double excitation part of the eigenvectors is treated at a higher level than the ground state amplitudes (vide infra). Thus, it might be the case that for higher-order methods beyond ADC(2)-x, which treat excited and ground state amplitudes on the same footing, the PNO truncation errors are again smaller than for PNO-ADC(2)-x. Taking this into account, it is very encouraging that a threshold of 10^{-7} is still sufficient to converge the PNO-ADC(2)-x excitation energies reliably within 0.1 eV, which is much below the inherent errors of ADC(2)-x, and will also be sufficient for a future PNO implementation of CCSD and related methods. Only for methods which include connected triple excitations and have smaller inherent errors, as e.g. CCSDR(3) and CC3, an improved convergence with T_{PNO} and thus with the size of the PNO expansion would be desirable.

To demonstrate the computational performance of the PNO implementation of ADC(2)-x, we compare in Fig. 2 the wall time for PNO-ADC(2)-x with that for canonical ADC(2)-x calculations for a series of polyenes C_nH_{n+2} in the all-trans configurations with a threshold of $T_{\mathrm{PNO}} = 10^{-8}$. As mentioned in Section 2, our current implementation of PNO-ADC(2)-x still contains for the PNO construction and the generation and transformation of the required 3-index integrals some steps with cubic and quartic cost-scalings. The most expensive of these steps is the generation of the integrals

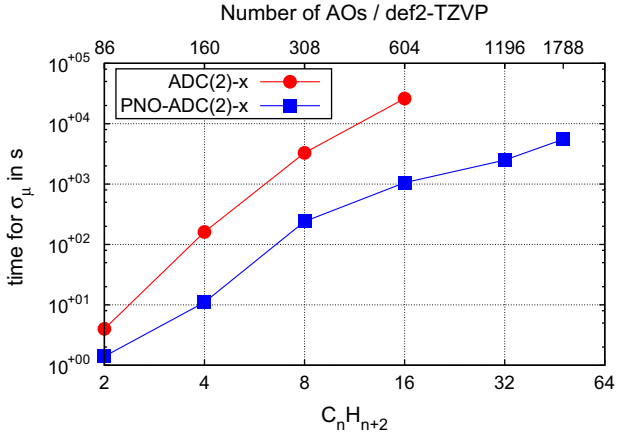


Fig. 2. Timings for a single transformation with the secular matrix **M** in canonical ADC(2)-x and PNO-ADC(2)-x with $T_{\mathrm{PNO}} = 10^{-8}$ on conjugated polyene chains C_nH_{n+2}.

for $\langle\mu_2|[H-F,\tau_2]|\mathrm{HF}\rangle$. This can, however, be done before the iterative solution of the eigenvalue problem because the compact PNO representation makes it feasible to precompute and store these integrals. We thus see for the linear transformations with the secular matrix **M** for small systems a quartic cost-scaling which decreases in the intermediate region between 300 and 1200 basis function to an almost quadratic scaling before the steps with cubic and quartic cost scaling become time determining. The canonical implementation has a much higher prefactor. In the regime $\lessapprox$600 basis functions its costs are dominated by the evaluation of the 4-index integrals in the AO basis $(\mu\nu|\kappa\lambda)$ and their contraction with the doubles amplitudes in the contravariant AO basis $\sum_{\mu\kappa} t^{ij}_{\mu\kappa}(\mu\nu|\kappa\lambda)$. These steps have operation counts that would formally scale with N^4 and O^2N^4, but can be reduced with the usual Schwarz screening [52] to a quadratic scaling for the AO integral evaluation and a quartic scaling for the contraction. The curve in Fig. 2 reflects the intermediate scaling of the costs in the regime of less than 600 AO basis functions. For larger systems the computational time will for the canonical implementation be dominated by the ring term contribution to $\langle\mu_2|[H-F,\tau_2]|\mathrm{HF}\rangle$, which exhibits also in the ricc2 code the well-known cost-scaling with O^3V^3. Calculations with canonical implementations of ADC(2)-x become, similar as for CCSD and related methods, for systems with more than 20 atoms soon intractable if point group symmetry cannot be used to reduce the prefactor. Because of the steep cost scaling, also a parallelization would help little to extent the applicability of these methods. The PNO implementation clearly paves the way for excitation energy calculations with such higher-order methods on larger systems. Already with our preliminary implementation the PNO-ADC(2)-x calculation for $C_{32}H_{34}$ is faster than the canonical calculation on C_8H_{10} which is four times smaller. The calculations on the largest system, $C_{48}H_{50}$ with 98 atoms and 1788 basis functions, is for the canonical implementation already out of reach without parallelization.

5. Comparison of ADC(2)-x with ADC(2)-s and the CC methods CCSD and CC3

Although ADC(2)-x has been advocated and applied in several studies [31,32,53]—in particular to molecules with non-negligible double excitation contributions in low-lying excited states—the method has never been benchmarked for a broader test set in comparison to accurate reference data obtained in the same basis set. For the test set developed by Schreiber et al. vertical excitation energies obtained with the approximate coupled cluster singles, doubles, and triples method CC3 and multi-state complete active space perturbation theory through second order, MS-CASPT2, in the TZVP basis and for the same structures used in the current work are available from Ref. [48]. From the canonical reference calculations done for the comparison in the previous section we have for the 102 singlet excitations in this test set also the corresponding ADC(2)-x results available. Fig. 3 shows a comparison of the deviations from the CC3 reference values for the extended and the strict ADC(2) methods, two perturbative modifications of ADC(2)-x (vide infra), and CCSD. By comparing with results from higher level calculations obtained with the same basis set and at the same geometry, we ensure that the deviations are exclusively caused by the electronic structure method. As concluded by Silva-Junior et al. [54], CC3 is currently the most reliable benchmark method applicable for this large test set apart for states with single excitation weights of less than 80% where the MS-CASPT2 results might be more accurate. But even in the latter case the differences between the CC3 and MS-CASPT2 values are usually small compared to the deviations of the methods studied here. Anyway, Table 1 summarizes in addition to the mean errors, standard

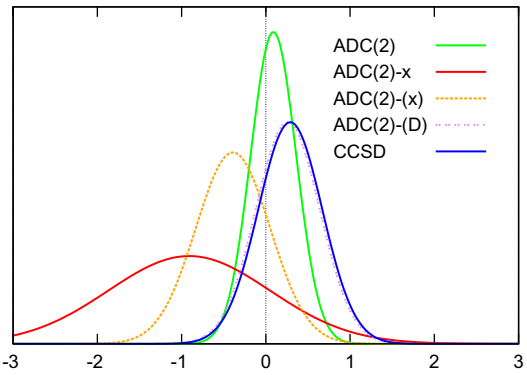


Fig. 3. Comparison of the deviations of 102 singlet excitation energies (in eV) computed in the TZVP basis set from the CC3 reference values taken from Ref. [48]. The center of the Gaussian distributions indicates the mean error and their width the standard deviation.

deviations, mean absolute and maximum errors relative to CC3 also the respective results of the analysis with the MS-CASPT2 values as reference. The results show clearly that ADC(2)-x does in general not improve excitation energies relative to the results obtained with the strict second-order model ADC(2)-s. In fact, ADC(2)-x provides from all methods included in this comparison overall the least accurate results, which are not only significantly red shifted by on average 0.91 eV relative to CC3 (and 0.73 eV relative to CASPT2), but has with 0.96 and 0.82 eV also the largest standard deviations. From the methods included in this test the strict second-order model ADC(2)-s agrees best with the CC3 reference, even better than the formally more complete CCSD model. This is connected to the close relation between ADC(2) and the approximate singles and doubles method CC2 which gives in general very similar excitation energies and was already found in Refs. [48,49] to agree for organic molecules with single reference ground states better with CC3 than CCSD. It is most surprising that the difference in accuracy, in particular in the mean absolute errors and the standard deviations, between ADC(2)-x and ADC(2)-s is so much larger than between ADC(2)-s and CCSD irrespectively whether we compare with the CC3 or the CASPT2 reference values.

6. Origin of the red shift of ADC(2)-x excitation energies

That the inclusion of the first-order matrix elements in the 2*p*–2*h* block of the secular matrix for ADC(2)-x leads to a substantial red shift of all excitation energies has been observed before by other authors [30,56,57]. Already Trofimov and Schirmer noted this trend when they proposed [30] this approximation in 1995 as an extension of ADC(2) which describes doubly excited states correct through first order in the fluctuation potential. Usually, this red shift is attributed to an overestimation of the influence of doubly-excited states [31,57]. Consequently, Krauter et al. studied recently how the accuracy and the computational performance of ADC(2)-x can be enhanced by an empirical down-scaling of the doubles contribution, which was inspired by the scaled opposite spin (SOS) variants of MP2 [38], CIS(D) [39], and ADC(2)-s [40]. But the empirical scaling led only to a limited improvement of the accuracy of ADC(2)-x and the SOS approximation has in addition the disadvantage that it entirely neglects certain classes of doubly excited configuration state functions, which is problematic for a method that aims at the description of doubly excited states.

Table 1
Mean errors (MEs), mean absolute errors (MAEs), standard deviation (SD), and maximum errors (MAX) of 102 vertical singlet excitation energies in eV with several ADC and CC methods compared to CC3 and, in parenthesis, the corresponding values for the comparison with MS-CASPT2. For details see supplementary material [55].

Method	ME	MAE	SD	MAX
CCSD	+0.29 (+0.47)	0.29 (0.48)	0.38 (0.57)	1.28 (1.62)
ADC(2)-x	+0.91 (−0.73)	0.92 (0.75)	0.96 (0.82)	1.75 (1.71)
ADC(2)	+0.09 (+0.27)	0.17 (0.31)	0.27 (0.41)	1.00 (1.30)
ADC(2)-(D)	+0.26 (+0.44)	0.29 (0.46)	0.38 (0.56)	1.24 (1.68)
ADC(2)-(x)	−0.39 (−0.21)	0.41 (0.28)	0.44 (0.34)	0.73 (0.77)

The hierarchies of algebraic-diagrammatic construction and coupled cluster response methods for excitation energies share a common first-order model for single excitations: ADC(1) and coupled cluster singles (CCS) are both for excitation energies (although not for other properties) equivalent to configuration interaction singles (CIS), with the secular matrix given by

$$\mathbf{M}^{(1)}_{\mu_1,\nu_1} = \langle \mu_1 | H - E_{\mathrm{HF}} | \nu_1 \rangle = \langle \mu_1 | [H, \tau_{\nu_1}] | \mathrm{HF} \rangle = \mathbf{A}^{(1)}_{\mu_1,\nu_1}. \tag{20}$$

The CIS (or ADC(1) or CCS) eigenvectors and excitation energies are usually used as zeroth-order approximation, $\mathbf{E}^{(0)}$ and $\omega^{(0)}$, for a perturbation expansion [16] of the exact eigenvectors and excitation energies. Within both approaches the first-order correlation correction to the eigenvectors is given by

$$E^{(1)}_{\mu_2} = -\left(\mathbf{A}^{(0)} - \omega^{(0)}\mathbf{1}\right)^{-1}_{\mu_2\nu_2} \mathbf{A}^{(1)}_{\nu_2\kappa_1} E^{(0)}_{\kappa_1}, \tag{21}$$

where the zeroth-order secular matrix (or Jacobian) contains the matrix elements over the Fock operator $\mathbf{A}^{(0)}_{\mu\nu} = \mathbf{M}^{(0)}_{\mu\nu} = \langle \mu | [F, \tau_\nu] | \mathrm{HF} \rangle$ and the first-order coupling elements between the *p*–*h* and 2*p*–2*h* spaces are given by $\mathbf{A}^{(1)}_{\mu_2\nu_1} = \mathbf{M}^{(1)}_{\mu_2\nu_1} = \langle \mu_2 | [H, \tau_{\nu_1}] | \mathrm{HF} \rangle$. Again, these matrix elements are identical for the algebraic-diagrammatic construction and for coupled cluster response theory. For both approaches the second-order correlation correction to the excitation energy is identical with the perturbative doubles correction to configuration interaction singles, CIS(D), introduced by Head-Gordon et al. [16],

$$\omega^{(2)} = \mathbf{E}^{(0)\dagger}_{\mu_1} \left(\mathbf{A}^{(1)}_{\mu_1\nu_2} \mathbf{E}^{(1)}_{\nu_2} + \mathbf{A}^{(2)}_{\mu_1\nu_1} \mathbf{E}^{(0)}_{\nu_1} \right), \tag{22}$$

because the second-order contributions to the *p*–*h* blocks in ADC and CC response theory are related [58] by $\mathbf{M}^{(2)}_{\mu_1\nu_1} = \frac{1}{2}\left(\mathbf{A}^{(2)}_{\mu_1\nu_1} + \mathbf{A}^{(2)}_{\nu_1\mu_1}\right)$. But the corresponding iterative second-order methods for single excitations, ADC(2) and CIS(D_∞), are different because the Jacobi matrix for CIS(D_∞) is, similar as for CC2 and higher-order CC methods, not hermitian. An analysis [59] of the two contributions to the second-order correction for single excitation energies reveals that the first term in Eq. (22),

$$\omega^{(2)}_{es} = \langle E^{(0)\dagger}_1 | [H, E^{(1)}_2] | \mathrm{HF} \rangle, \tag{23}$$

which depends on the double excitation part of the eigenvector, accounts for correlation effects in the excited state, which lower the excitation energies, while the second term in Eq. (22)

$$\omega^{(2)}_{gs} = \langle E^{(0)\dagger}_1 | [[H, T^{(1)}_2], E^{(0)}_1] | \mathrm{HF} \rangle \tag{24}$$

accounts for correlation effects in the ground state, which increase the excitation energies. Since the two contributions are usually of similar magnitude, often in the order of 0.3–3 eV, the net effect of $\omega^{(2)} = \omega^{(2)}_{es} + \omega^{(2)}_{gs}$ depends crucially on the balance of the two contributions.

The first-order contribution to the 2*p*–2*h* block of the secular matrix, which is added in the extended ADC(2) approximation, introduces for singly excited states a third-order correction

$$\omega^{(3)}_{es} = \langle E^{(1)\dagger}_2 | [H - F, E^{(1)}_2] | \mathrm{HF} \rangle, \tag{25}$$

which accounts for similar correlation effects in the excited state as the related third-order Møller–Plesset (MP3) correction

$$E_{\mathrm{MP3}} = \langle T^{(1)\dagger}_2 | [H - F, T^{(1)}_2] | \mathrm{HF} \rangle \tag{26}$$

does for the ground state energy. Consequently, the contribution $\omega_{es}^{(3)}$ usually lowers the excitation energies. The red shift can be significant even for single excitation dominated transitions and without that large changes in the eigenvectors would be required. This is clearly seen when the direct contribution from this term is evaluated with the ADC(2)-s eigenvectors as perturbative "double excitation correction", ADC(2)-(x), to the strict second order ADC(2) excitation energies:

$$\omega_{es}^{(x)} = \langle E_2^{\mathrm{ADC}(2)\dagger} | [H - F, E_2^{\mathrm{ADC}(2)}] | \mathrm{HF} \rangle \tag{27}$$

$$\omega^{\mathrm{ADC}(2)-(x)} = \omega^{\mathrm{ADC}(2)-s} + \omega_{es}^{(x)} \tag{28}$$

In the iterative ADC(2)-x model the red shift is enhanced because of the variational optimization of the eigenvectors and the accuracy deteriorates even more so that the absolute accuracy of the ADC(2)-x excitation energies is, at least for the test set from Schreiber et al. [48,49], not much better than for CIS excitation energies.

Similar as $\omega_{es}^{(2)}$ also $\omega_{es}^{(3)}$ is accompanied by a corresponding term which accounts for related correlation effects in the ground state wavefunction. It appears in the coupling between the p–h and the $2p$–$2h$ blocks, i.e. within the ADC approach in $\mathbf{M}^{(2)}_{\mu_1 \nu_2}$ and $\mathbf{M}^{(2)}_{\mu_2 \nu_1}$ and in coupled cluster response theory in $\mathbf{A}^{(2)}_{\mu_2 \nu_1}$. Since the derivation of the third-order contribution within ADC is rather lengthy [60], we only motivate the missing coupling term by comparison with CC response theory. The usual approach taken in CC response theory is to start from the cluster equations of a ground state model which includes all required terms and to derive from them by differentiation with respect to the cluster amplitudes the corresponding Jacobian. Since we aim for an approximation which is correct through second order for single excitations and correct through first order for double excitations, we can start from LCCSD- or CEPA(0)-like equations where we keep similar as in the derivation of CC2 and CC3, all nonlinear terms that arise from the singles amplitudes since they play a crucial role in response theory. With the short-hand notation $\widetilde{H} = \exp(-T_1) H \exp(T_1)$ we can write them as:

$$0 = \langle \mu_1 | \widetilde{H} + [\widetilde{H}, T_2] | \mathrm{HF} \rangle, \tag{29}$$

$$0 = \langle \mu_2 | \widetilde{H} + [\widetilde{H}, T_2] | \mathrm{HF} \rangle. \tag{30}$$

This leads to the Jacobi matrix:

$$\begin{pmatrix} \langle \mu_1 | [\widetilde{H}, \tau_{\nu_1}] + [[\widetilde{H}, T_2], \tau_{\nu_1}] | \mathrm{HF} \rangle & \langle \mu_1 | [\widetilde{H}, \tau_{\nu_2}] | \mathrm{HF} \rangle \\ \langle \mu_2 | [\widetilde{H}, \tau_{\nu_1}] + [[\widetilde{H}, T_2], \tau_{\nu_1}] | \mathrm{HF} \rangle & \langle \mu_2 | [\widetilde{H}, \tau_{\nu_2}] | \mathrm{HF} \rangle \end{pmatrix}. \tag{31}$$

If we now skip the contributions from the ground state singles amplitudes T_1, which in second order do not contribute to the excitation energies of both singly and doubly excited states, we arrive at a Jacobi matrix

$$\begin{pmatrix} \langle \mu_1 | [H, \tau_{\nu_1}] + [[H, T_2], \tau_{\nu_1}] | \mathrm{HF} \rangle & \langle \mu_1 | [H, \tau_{\nu_2}] | \mathrm{HF} \rangle \\ \langle \mu_2 | [H, \tau_{\nu_1}] + [[H, T_2], \tau_{\nu_1}] | \mathrm{HF} \rangle & \langle \mu_2 | [H, \tau_{\nu_2}] | \mathrm{HF} \rangle \end{pmatrix}, \tag{32}$$

which differs from the secular matrix of ADC(2)-x only in two aspects:

- The second-order contribution to the diagonal p–h block $\mathbf{A}^{(2)}_{\mu_1 \nu_1} = \langle \mu_1 | [[H, T_2], \tau_{\nu_1}] | \mathrm{HF} \rangle$ is not symmetrized.
- The $2p$–$2h$/p–h coupling block contains the additional second-order matrix elements $\mathbf{A}^{(2)}_{\mu_2 \nu_1} = \langle \mu_2 | [[H, T_2], \tau_{\nu_1}] | \mathrm{HF} \rangle$ which account for the influence of additional correlation effects in the ground state wavefunction on the excitation energies that we seek for. It has its origin in the contributions of $\langle \mu_2 | [\widetilde{H}, T_2] | \mathrm{HF} \rangle$ to the cluster equations as does the commutator $\langle \mu_2 | [H - F, \tau_{\nu_2}] | \mathrm{HF} \rangle$ which is added in ADC(2)-x.

In the hermitian secular matrix of the full ADC(3) method the contributions from $\mathbf{A}^{(2)}_{\mu_2 \nu_1}$ appear with a pre-factor of $\frac{1}{2}$ in $\mathbf{M}^{(2)}_{\mu_2 \nu_1}$ and again with a pre-factor of $\frac{1}{2}$ in adjoint form in $\mathbf{M}^{(2)}_{\mu_1 \nu_2}$. ADC(3) also includes some other third-order terms to achieve a perturbation theoretical consistency through third order for dominantly singly excited states. We aim here, however, for a simple extension of ADC(2) which describes double excitations correct through first order and retains in difference to ADC(2)-x at least approximately the second order accuracy of ADC(2)-s for single excitations. In cases where single and double excitations are important and should be considered as zero-order parameters, the coupling blocks $\mathbf{A}^{(2)}_{\mu_2 \nu_1}$ and $\mathbf{A}^{(2)}_{\mu_1 \nu_2}$ contribute already in second-order to the excitation energies. ADC(2)-x, which neglects these matrix elements, is then also for single excitations similar as CIS only consistent through first-order in the fluctuation potential, while a method which includes in addition these terms will be still formally consistent through second-order for single excitations, similar as ADC(3) and CCSD.

To demonstrate the effect of the above discussed coupling terms, we evaluate them again as perturbative correction to the strict ADC(2) method—an approximation which we denote in the following as ADC(2)-(D):

$$\omega_{gs}^{(D)} = \langle E_2^{\mathrm{ADC}(2)\dagger} | [[H, T_2^{(1)}], E_1^{\mathrm{ADC}(2)}] | \mathrm{HF} \rangle \tag{33}$$

$$\omega^{\mathrm{ADC}(2)-(\mathrm{D})} = \omega^{\mathrm{ADC}(2)-s} + \omega_{es}^{(x)} + \omega_{gs}^{(D)} \tag{34}$$

The correction term $\omega_{gs}^{(D)}$ can be computed with techniques developed for CCSD response calculations, e.g. using the formulation described in Ref. [61]. The costs scale as for $\omega_{es}^{(x)}$ in a canonical implementation with the sixth power of the system size. But if evaluated for several states the pre-factor for $\omega_{gs}^{(D)}$ is smaller than for $\omega_{es}^{(x)}$ because one can partially exploit pre-contracted matrix elements for $[H, T_2^{(1)}]$ as state-independent intermediates. In a PNO-oriented framework $\omega_{gs}^{(D)}$ can be implemented with a mixture of the techniques described recently by the Neese group [29,44] for LPNO-CCSD and by ourself for PNO-MP3-F12 [35].

As the results in Fig. 3 clearly demonstrate, the contribution form $[H, T_2]$ to the $2p$–$2h$/$1p$–$1h$ coupling term increases the excitation energies. Similar as for the strict second-order methods, the contributions from the ground and the excited state double excitations often cancel each other to a large extent. But in most cases, $\omega_{gs}^{(D)}$ is larger than $\omega_{es}^{(x)}$ so that the net effect is a slight blue shift relative to ADC(2)-s. The perturbative ADC(2)-(D) results are surprisingly close to those from the CCSD method. In Fig. 3 the curves for CCSD and ADC(2)-(D), which represent the mean error and the standard deviation of the errors, are almost on top of each other. A typical example is naphthalene for which we collected the results in Table 2. A graphical overview of the excitation energies is shown in Fig. 4. For all of the ten lowest excitations included in the test set the ADC(2)-(D) results are within 0.15 eV of the excitation energies obtained with CCSD, even if the individual contributions from $\omega_{es}^{(x)}$ and $\omega_{gs}^{(D)}$ are larger than 0.8 eV as for the 3 ^1A_g and 3 $^1B_{3u}$ states. The excitation energies obtained with the iterative ADC(2)-x method are in all cases too low. The red shift relative to the CC3 reference results increases with the contribution of double excitations to the transition, $\%E_2$, but is for all excited states of naphthalene relatively large, between 0.57 eV for 2 $^1B_{1g}$ with 8.7 $\%E_2$ and 1.44 eV for 3 $^1B_{3u}$ with 46.3 $\%E_2$. The large variations in the red shift leads to a wrong ordering of excited states even if they are not nearly degenerate. In naphthalene ADC(2)-x predicts the 3 ^1A_g state below the 2 $^1B_{2u}$ and 2 $^1B_{1g}$ states, while all other methods, including CASPT2, predict it above these states. We must thus conclude that the results obtained with the iterative ADC(2)-x method are not only red shifted but that also the magnitude of the red shifts depends strongly on the character of the excited state so that—at least for closed-shell molecules—its predictive capability (measured by the STD of the errors in Table 1) is not better than for CIS.

Table 2
Vertical excitation energies ω in eV and percentage of doubles $\%E_2$ in excited state amplitudes computed with several ADC and CC methods for the lowest singlet states in naphthalene with the TZVP basis set.

State	CASPT2	CC3		CC2		CCSD		ADC(2)-x		ADC(2)-s		ADC(2)-(D)	ADC(2)-(x)
	ω	ω	$\%E_2$	ω	$\%E_2$	ω	$\%E_2$	ω	$\%E_2$	ω	$\%E_2$	ω	ω
$1\,^1B_{3u}$	4.24	4.27	14.8	4.45	8.5	4.41	9.5	3.45	18.0	4.46	10.4	4.54	3.96
$1\,^1B_{2u}$	4.77	5.03	9.4	4.96	6.9	5.21	5.8	4.33	11.6	4.94	9.2	5.14	4.59
$2\,^1A_g$	5.87	5.98	17.8	6.22	8.6	6.23	10.3	4.94	35.6	6.23	10.8	6.32	5.69
$1\,^1B_{1g}$	5.99	6.07	20.4	6.21	9.3	6.53	8.7	5.08	26.7	6.23	12.1	6.46	5.74
$2\,^1B_{3u}$	6.06	6.33	9.3	6.25	7.0	6.55	6.2	5.59	11.7	6.23	9.6	6.53	5.86
$2\,^1B_{2u}$	6.33	6.57	9.5	6.57	6.7	6.77	6.2	5.92	11.3	6.55	9.0	6.77	6.19
$2\,^1B_{1g}$	6.47	6.79	8.7	6.82	6.0	6.98	6.3	6.22	10.3	6.80	7.8	6.92	6.43
$3\,^1A_g$	6.67	6.90	30.0	7.34	11.5	7.77	13.2	5.67	41.4	7.38	15.6	7.65	6.77
$3\,^1B_{2u}$	7.74	8.44	12.1	8.46	7.2	8.77	6.6	7.70	15.8	8.46	9.5	8.66	8.03
$3\,^1B_{3u}$	8.17	8.12	46.3	8.85	12.8	9.03	16.1	6.68	51.1	8.89	14.8	9.00	8.14

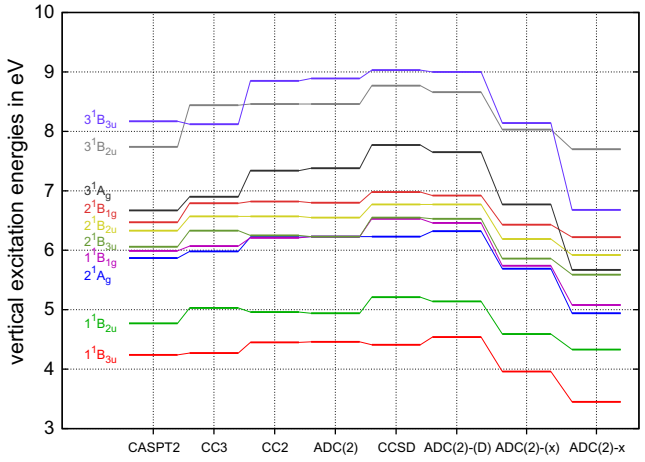


Fig. 4. A comparison of the results for the 10 lowest vertical excitations in naphthalene.

From the methods studied here, the perturbative ADC(2)-(x) model gives for the states with the largest double excitation contributions ($3\,^1A_g$ and $3\,^1B_{3u}$) results that are closest to the CC3 and CASPT2 reference values. But similar as the iterative ADC(2)-x model it gives for single excitation dominated transitions ($1\,^1B_{2u}$, $2\,^1B_{3u}$, $2\,^1B_{2u}$, $2\,^1B_{1g}$) unbalanced red shifted results. The ADC(2)-(D) results exhibit on average a blue shift compared to the CC3 reference values, which is largest for the two states with the largest double excitation weights $3\,^1A_g$ and $3\,^1B_{3u}$. The origin for this is that triple excitations are needed to describe correctly the first-order correlation correction of eigenvectors for excited states with a large double excitation contribution:

$$E^{(1)}_{\mu_i} = -\sum_{i=1,2,3} \left(\mathbf{A}^{(0)} - \omega^{(0)}\mathbf{1}\right)^{-1}_{\mu_i\nu_i} \mathbf{A}^{(1)}_{\nu_i\kappa_2} E^{(0)}_{\kappa_2} \tag{35}$$

The terms that result from $E^{(1)}_{\mu_3}$ are the most important contribution for excitation energies of doubly excited states beyond CCSD and, in fact, the only contribution included in the CCSDR(T) perturbative correction [62], which approximates CC3 usually well.

That the ADC(2)-(D) results are consistently close to the CCSD values indicates that at this level the effects from the solution of the eigenvalue problem (instead of a perturbative correction) and the additional higher-order singles and doubles terms, in which the two methods differ, are small compared to the triples corrections.

The conclusion from these results is thus that for molecules with single-reference closed-shell ground states only such ab initio wavefunction methods will be able to improve the results for vertical excitation energies systematically upon those obtained with CC2 or ADC(2)-s which account for connected triple excitations either in a single-reference scheme, as CCSDR(T), CCSDR(3), or CC3 do, or in a multi-reference setup. The inclusion of higher-order contributions in the diagonal and off-diagonal $2p$–$2h$ and $1p$–$1h$ blocks of the secular or Jacobi matrix as in ADC(2)-(x), ADC(2)-(D), and CCSD provides only a qualitative description of double excitations, which can be used to study certain trends but not to obtain quantitative results.

A slight further improvement can be obtained by mimicking the missing (excitation energy lowering) contribution from $E^{(1)}_{\mu_3}$ by an empirical down-scaling of the $\omega^{(D)}_{gs}$ correction term: Optimization of the weight for $\omega^{(D)}_{gs}$ by minimization of the MAE relative to CC3 results in a prefactor of $\approx 2/3$ and a MAE of 0.16 eV. The smallest MAE relative to CASPT2 (0.21 eV) is obtained with a weight of $\approx 1/3$. This shows the limitations of such a procedure. Our recommendation is to use a weight of 1/2 (with a MAE of 0.18 eV relative to CC3 and 0.23 eV relative to CASPT2) with $\pm 0.5\omega^{(D)}_{gs}$ as an estimate for the remaining uncertainty.

7. Summary and conclusions

The results presented in Section 4 for the extended second-order ADC method ADC(2)-x demonstrate that the truncated pair natural orbital expansion with state-specific PNOs opens a new perspective to implement response methods beyond ADC(2)-s and CC2 with a reduced cost-scaling. Already with our initial implementation we obtain for the linear transformations with the secular matrix a reduction of the computational costs by a factor of 10–30 for medium sized molecules. Because of the reduced scaling the savings increase further with increasing system size. For the largest calculations reported here the wall time for the linear transformations with the secular matrix are already shorter than for canonical calculations on four times smaller systems. This makes these methods already applicable to four times larger systems.

The inclusion of the first-order coupling between doubles $\mathbf{A}^{(1)}_{\mu_2\nu_2} = \langle\mu_2|[H-F,\nu_2]|\mathrm{HF}\rangle$ leads—despite much larger contributions from double excitations to the eigenvectors and the excitation energies—only to a modest increase of the PNO truncation errors by a factor of 2–5. A truncation threshold of 10^{-7} is still sufficient to converge the excitation energies securely within 0.1 eV. With a threshold of 10^{-8} the maximum errors are already below 0.03 eV, which would even be sufficient for methods that include connected triple excitations as e.g. CCSDR(3) and CC3. But at this level excitation energies would probably be sufficiently accurate if only the CCSD eigenvalue problem is solved with a large PNO basis obtained with such a tight threshold. A more compact PNO basis for

the CCSDR(3) or CC3 calculation could then be generated from the CCSD eigenvectors.

Despite promising results reported recently in the literature [31,32] for the extended second-order model ADC(2)-x, the comparison with accurate CC3 and CASPT2 results for a large test set of 102 singlet excitations in organic molecules reveals an unbalanced description of correlation effects by the method. The mean errors and the standard deviations are much larger than for strict second-order methods as ADC(2)-s and CC2, almost in the same ball park as CIS. Even for states with large contributions from doubly excited configurations, which are only poorly described by ADC(2)-s or CC2, the excitation energies are not improved with ADC(2)-x; the errors have just the opposite sign. An analysis presented in Section 6 shows that the reason for the large underestimation of the excitation energies in ADC(2)-x are the missing second-order coupling elements between the $1p$–$1h$ and $2p$–$2h$ spaces, which account for correlation effects in the ground state. Inclusion of these matrix elements reestablishes the balance between ground and excited state correlation effects. As a result we could devise a perturbative double excitation correction for ADC(2)-s which gives excitation energies close to those of the CCSD model, but has, because of its perturbative nature, already with a canonical implementation much lower computational costs. The size of these corrections is an indicator for the importance of double excitations for excitation energies. To improve the results for excitation energies systematically upon those obtained with ADC(2) and CC2 requires, however, the inclusion of connected triples since the leading-order triples correction to the excitation energies is of the same order of magnitude as the errors of the second-order methods ADC(2) and CC2 and can hardly be mimicked by an empirical scaling of contributions from the single or double excitation amplitudes. This is a challenge for the development of wavefunction methods for excited states that surpass these second-order methods systematically in accuracy but are still applicable to large molecules with 50–100 or more atoms.

We could devise two perturbative corrections to ADC(2), denoted ADC(2)-(x) and ADC(2)-(D), which provide in most cases lower and upper bounds for the excitation energies and approximate the CC3 and CASPT2 reference results better than CCSD and ADC(2)-x, while they are about an order of magnitude cheaper than the latter two methods. The size of the (x) and (D) perturbative corrections is a more robust indicator for the remaining errors of the ADC(2) and CC2 methods than the usual weight of the doubles in the eigenvectors.

The development of a fully PNO-based implementation of CCSD and approximate triples methods for excitation energies will be subject of forthcoming work in our group.

Acknowledgment

The authors acknowledge support by the Deutsche Forschungsgemeinschaft (DFG) through Grant No. HA 2588/7-1.

Appendix A. Supplementary material

Supplementary data associated with this article can be found, in the online version, at http://dx.doi.org/10.1016/j.comptc.2014.03.004.

References

[1] J.F. Stanton, J. Gauss, Analytic energy gradients for the equation-of-motion coupled-cluster method: implementation and application to the HCN/HNC system, J. Chem. Phys. 100 (1994) 4695–4698.
[2] N. Ishikawa, M. Head-Gordon, Analytical gradient of the CIS(D) perturbative correction to single-excitation configuration-interaction excited-states, Int. J. Quantum Chem. Symp. 29 (1995) 421–427.
[3] C. van Caillie, R. Amos, Geometric derivatives of excitation energies using SCF and DFT, Chem. Phys. Lett. 308 (1999) 249–255.
[4] C. van Caillie, R. Amos, Geometric derivatives of density functional theory excitation energies using gradient-corrected functionals, Chem. Phys. Lett. 317 (2000) 159–164.
[5] F. Furche, R. Ahlrichs, Adiabatic time-dependent density functional methods for excited state properties, J. Chem. Phys. 117 (2002) 7433–7447.
[6] A. Köhn, C. Hättig, Analytic gradients for excited states in the coupled-cluster model CC2 employing the resolution-of-the-identity approximation, J. Chem. Phys. 119 (2003) 5021–5036.
[7] H. Hettema, H.J.A. Jensen, P. Jørgensen, J. Olsen, Quadratic response functions for a multiconfigurational self-consistent field wave function, J. Chem. Phys. 97 (1992) 1174–1190.
[8] D. Sundholm, A. Rizzo, P. Jørgensen, Multiconfiguration self-consistent field quadratic response calculations of the two-photon transition probability rate constants for argon, J. Chem. Phys. 101 (1994) 4931–4935.
[9] D. Sundholm, J. Olsen, P. Jørgensen, A multiconfiguration self-consistent-field response study of one- and two-photon dipole transitions between the $X^1\Sigma^+$ and $A^1\Pi$ states of CO, J. Chem. Phys. 102 (1995) 4143–4150.
[10] M.J. Paterson, O. Christiansen, F. Pawłowski, P. Jørgensen, C. Hättig, T. Helgaker, P. Sałek, Benchmarking two-photon absorption with CC3 quadratic response theory, and comparison with density-functional response theory, J. Chem. Phys. 124 (2006) 054322.
[11] C. Hättig, O. Christiansen, P. Jørgensen, Multiphoton transition moments and absorption cross section in coupled cluster response theory employing variational transition moment functionals, J. Chem. Phys. 108 (1998) 8331–8354.
[12] D.H. Friese, C. Hättig, K. Ruud, Calculation of two-photon absorption strengths with the approximate coupled cluster singles and doubles model CC2 using the resolution-of-identity approximation, Phys. Chem. Chem. Phys. 14 (2012) 1175–1184.
[13] O. Christiansen, First-order nonadiabatic coupling matrix elements using coupled cluster methods. I. Theory, J. Chem. Phys. 110 (1999) 711–723.
[14] A. Tajti, P.G. Szalay, Analytic evaluation of the nonadiabatic coupling vector between excited states using equation-of-motion coupled-cluster theory, J. Chem. Phys. 131 (2009) 124104.
[15] R. Send, F. Furche, First-order nonadiabatic couplings from time-dependent hybrid density functional response theory: consistent formalism, implementation, and performance, J. Chem. Phys. 132 (2010) 044107.
[16] M. Head-Gordon, R.J. Rico, M. Oumi, T.J. Lee, A doubles correction to electronic excited-states from configuration-interaction in the space of single substitutions, Chem. Phys. Lett. 219 (1994) 21–29.
[17] J. Schirmer, Beyond the random phase approximation: a new approximation scheme for the polarization propagator, Phys. Rev. A 26 (1981) 2395–2416.
[18] O. Christiansen, H. Koch, P. Jørgensen, The second-order approximate coupled cluster singles and doubles model CC2, Chem. Phys. Lett. 243 (1995) 409–418.
[19] C. Hättig, F. Weigend, CC2 excitation energy calculations on large molecules using the resolution of the identity approximation, J. Chem. Phys. 113 (2000) 5154–5161.
[20] D. Kats, T. Korona, M. Schütz, Local CC2 electronic excitation energies for large molecules with density fitting, J. Chem. Phys. 125 (2006) 104106.
[21] D. Kats, M. Schütz, A multistate local coupled cluster CC2 response method based on the Laplace transform, J. Chem. Phys. 131 (2009) 124117.
[22] B. Helmich, C. Hättig, Local pair natural orbitals for excited states, J. Chem. Phys. 135 (2011) 214106.
[23] B. Helmich, C. Hättig, A pair natural orbital implementation of the coupled cluster model CC2 for excitation energies, J. Chem. Phys. 139 (2013) 084114.
[24] M. Head-Gordon, M. Oumi, D. Maurice, Quasidegenerate second-order perturbation corrections to single-excitation configuration interaction, Mol. Phys. 96 (1999) 593–602.
[25] T. Korona, H.-J. Werner, Local treatment of electron excitations in the EOM-CCSD method, J. Chem. Phys. 118 (2003) 3006–3019.
[26] T.D. Crawford, R.A. King, Locally correlated equation-of-motion coupled cluster theory for the excited states of large molecules, Chem. Phys. Lett. 366 (2002) 611–622.
[27] W. Meyer, Ionization energies of water from PNO-CI calculations, Int. J. Quantum Chem. 5 (1971) 341–348.
[28] F. Neese, F. Wennmohs, A. Hansen, Efficient and accurate local approximations to coupled-electron pair approaches: an attempt to revive the pair natural orbital method, J. Chem. Phys. 130 (2009) 114108.
[29] F. Neese, A. Hansen, D.G. Liakos, Efficient and accurate approximations to the local coupled cluster singles and doubles method using a truncated pair natural orbital basis, J. Chem. Phys. 131 (2009) 064103.
[30] A.B. Trofimov, J. Schirmer, An efficient polarization propagator approach to valence electron-excitation spectra, J. Phys. B 28 (1995) 2299–2324.
[31] J.H. Starcke, M. Wormit, J. Schirmer, A. Dreuw, How much double excitation character do the lowest excited states of linear polyenes have?, Chem Phys. 329 (2006) 39–49.
[32] S. Knippenberg, J.H. Starcke, M. Wormit, A. Dreuw, The low-lying excited states of neutral polyacenes and their radical cations: a quantum chemical study employing the algebraic diagrammatic construction scheme of second order, Mol. Phys. 108 (2010) 2801–2813.
[33] J. Yang, Y. Kurashige, F.R. Manby, G.K.L. Chan, Tensor factorizations of local second-order Møller–Plesset theory, J. Chem. Phys. 134 (2011) 044123.

[34] C. Krause, H.-J. Werner, Comparison of explicitly correlated local coupled-cluster methods with various choices of virtual orbitals, Phys. Chem. Chem. Phys. 14 (2012) 7591–7604.
[35] C. Hättig, D.P. Tew, B. Helmich, Local explicitly correlated second- and third-order Møller–Plesset perturbation theory with pair natural orbitals, J. Chem. Phys. 136 (2012) 204105.
[36] O. Vahtras, J. Almlöf, M. Feyereisen, Integral approximations for LCAO-SCF calculations, Chem. Phys. Lett. 213 (1993) 514–518.
[37] M. Feyereisen, G. Fitzgerald, A. Komornicki, Use of approximate integrals in ab initio theory. An application in MP2 energy calculations, Chem. Phys. Lett. 208 (1993) 359–363.
[38] Y. Jung, R.C. Lochan, A.D. Dutoi, M. Head-Gordon, Scaled opposite-spin second order Møller–Plesset correlation energy: an economical electronic structure method, J. Chem. Phys. 121 (2004) 9793–9802.
[39] Y.M. Rhee, M. Head-Gordon, Scaled second-order perturbation corrections to configuration interaction singles: efficient and reliable excitation energy methods, J. Phys. Chem. A 111 (2007) 5314–5326.
[40] A. Hellweg, S. Grün, C. Hättig, Benchmarking the performance of spin-component scaled CC2 in ground and electronically excited states, Phys. Chem. Chem. Phys. 10 (2008) 1159–1169.
[41] J. Almlöf, Elimination of energy denominators in Møller–Plesset perturbation theory by a Laplace transform approach, Chem. Phys. Lett. 181 (1991) 319–320.
[42] M. Häser, J. Almlöf, Laplace transform techniques in Møller–Plesset perturbation theory, J. Chem. Phys. 96 (1992) 489–494.
[43] G. Schmitz, B. Helmich, C. Hättig, A $\mathcal{O}(n^3)$ scaling PNO-MP2 method using a hybrid OSV-PNO approach with an iterative direct generation of OSVs, Mol. Phys. 111 (2013) 2463–2476.
[44] C. Riplinger, F. Neese, An efficient and near linear scaling pair natural orbital based local coupled cluster method, J. Chem. Phys. 138 (2013) 034106.
[45] Turbomole Development Version, 2013. For further information see <http://www.turbomole.com>.
[46] J. Pipek, P.G. Mezey, A fast intrinsic localization procedure applicable for ab initio and semiempirical linear combination of atomic orbital wave functions, J. Chem. Phys. 90 (1989) 4916–4926.
[47] TURBOMOLE V6.5, a development of University of Karlsruhe and Forschungszentrum Karlsruhe GmbH, 1989–2007, TURBOMOLE GmbH, since 2007; available from <http://www.turbomole.com>, 2013.
[48] M. Schreiber, M.R. Silva-Junior, S.P.A. Sauer, W. Thiel, Benchmarks for electronically excited states: CASPT2, CC2, CCSD, and CC3, J. Chem. Phys. 128 (2008) 134110.
[49] M.R. Silva-Junior, S.P. Sauer, M. Schreiber, W. Thiel, Basis set effects on coupled cluster benchmarks of electronically excited states: CC3, CCSDR(3) and CC2, Mol. Phys. 108 (2010) 453–465.
[50] A. Schäfer, C. Huber, R. Ahlrichs, Fully optimized contracted Gaussian basis sets of triple zeta valence quality for atoms Li to Kr, J. Chem. Phys. 100 (1994) 5829–5835.
[51] F. Weigend, M. Häser, H. Patzelt, R. Ahlrichs, RI-MP2: Optimized auxiliary basis sets and demonstration of efficiency, Chem. Phys. Lett. 294 (1998) 143–152.
[52] M. Häser, R. Ahlrichs, Improvements on the direct SCF method, J. Comp. Chem. 10 (1989) 104–111.
[53] J.H. Starcke, M. Wormit, A. Dreuw, Nature of the lowest excited states of neutral polyenyl radicals and polyene radical cations, J. Chem. Phys. 131 (2009) 144311.
[54] M.R. Silva-Junior, M. Schreiber, S.P. Sauer, W. Thiel, Benchmarks of electronically excited states: basis set effects on CASPT2 results, J. Chem. Phys. 133 (2010) 174318.
[55] 2013. See Supplemantary Material at URL.
[56] A.B. Trofimov, G. Stelter, J. Schirmer, Electron excitation energies using a consistent third-order propagator approach: comparison with full configuration interaction and coupled cluster results, J. Chem. Phys. 117 (2002) 6402–6410.
[57] C.M. Krauter, M. Pernpointner, A. Dreuw, Application of the scaled-opposite-spin approximation to algebraic diagrammatic construction schemes of second order, J. Chem. Phys. 138 (2013) 044107.
[58] C. Hättig, Structure optimizations for excited states with correlated second-order methods: CC2, CIS(D_∞), and ADC(2), Adv. Quantum Chem. 50 (2005) 37–60.
[59] H. Fliegl, C. Hättig, W. Klopper, Coupled-cluster response theory with linear-r_{12} corrections: the CC2-R12 model for excitation energies, J. Chem. Phys. 124 (2006) 044112.
[60] A.B. Trofimov, G. Stelter, J. Schirmer, A consistent third-order propagator method for electronic excitation, J. Chem. Phys. 111 (1999) 9982–9999.
[61] O. Christiansen, H. Koch, A. Halkier, P. Jørgensen, T. Helgaker, A.M. Sánchez de Merás, Large-scale calculations of excitation energies in coupled cluster theory: the singlet excited states of benzene, J. Chem. Phys. 105 (1996) 6921–6939.
[62] O. Christiansen, H. Koch, P. Jørgensen, Perturbative triple excitation corrections to coupled cluster singles and doubles excitation energies, J. Chem. Phys. 105 (1996) 1451–1459.